

The construction of a multifunctional luminescent Eu-MOF for the sensing of Fe^{3+} , $\text{Cr}_2\text{O}_7^{2-}$ and amines in aqueous solution

Cui-Li Wang, Ya-Xin Zheng, Le Chen, Cai-Yong Zhu, Wei Gao*, Peng Li, Jie-Ping Liu and Xiu-Mei Zhang*

Table S1 Selected bond lengths (\AA) and angles ($^\circ$) for **1-Eu**.

MOF	1-Eu
Eu1-O6A	2.300(3)
Eu1-O6B	2.300(3)
Eu1-O1C	2.310(3)
Eu1-O1	2.310(3)
Eu1-O9B	2.503(3)
Eu1-O9A	2.503(3)
Eu1-O10A	2.522(3)
Eu1-O10B	2.522(3)
Eu2-O7	2.369(3)
Eu2-O7D	2.369(3)
Eu2-O4D	2.546(3)
Eu2-O4	2.546(3)
Eu2-O12E	2.546(3)
Eu2-O12F	2.546(3)
Eu2-O3	2.555(3)
Eu2-O3D	2.555(3)
Eu2-O11E	2.607(3)
Eu2-O11F	2.607(3)
O6A-Eu1-O6B	96.58(16)
O6A-Eu1-O1C	156.09(12)
O6B-Eu1-O1C	93.73(11)
O6A-Eu1-O1	93.73(11)
O6B-Eu1-O1	156.09(12)
O1C-Eu1-O1	85.24(16)
O6A-Eu1-O9B	72.32(10)

O6B-Eu1-O9B	77.90(11)
O1C-Eu1-O9B	131.15(11)
O1-Eu1-O9B	84.82(12)
O6A-Eu1-O9A	75.86(12)
O6B-Eu1-O9A	123.98(11)
O1C-Eu1-O9A	131.15(11)
O1-Eu1-O9A	84.82(12)
O9B-Eu1-O9A	134.62(15)
O6A-Eu1-O10A	75.86(12)
O6B-Eu1-O10A	123.98(11)
O1C-Eu1-O10A	79.48(11)
O1-Eu1-O10A	80.47(12)
O9B-Eu1-O10A	143.33(10)
O9A-Eu1-O10A	51.71(9)
O6A-Eu1-O10B	123.98(10)
O6B-Eu1-O10B	75.86(12)
O1C-Eu1-O10B	80.47(12)
O1-Eu1-O10B	80.47(12)
O9B-Eu1-O10B	51.71(9)
O9A-Eu1-O10B	143.33(10)
O10A-Eu1-O10B	152.64(14)
O7-Eu2-O7D	139.89(17)
O7-Eu2-O4D	143.17(10)
O7D-Eu2-O4D	69.60(11)
O7-Eu2-O4	69.60(11)
O7D-Eu2-O4	143.17(10)
O4D-Eu2-O4	97.57(14)
O7-Eu2-O12E	88.36(12)
O7D-Eu2-O12E	87.70(12)
O4D-Eu2-O12E	119.87(11)
O4-Eu2-O12E	68.54(10)
O7-Eu2-O12F	87.70(12)
O7D-Eu2-O12E	88.36(12)
O4D-Eu2-O12F	68.54(10)

O4-Eu2-O12F	119.87(11)
O12E-Eu2-O12F	168.49(14)
O7-Eu2-O3	71.64(11)
O7D-Eu2-O3	142.14(11)
O4D-Eu2-O3	73.74(9)
O4-Eu2-O3	50.81(9)
O12E-Eu2-O3	119.33(11)
O12F-Eu2-O3	69.44(11)
O7-Eu2-O3D	142.14(10)
O7D-Eu2-O3D	71.64(11)
O4D-Eu2-O3D	50.81(9)
O4-Eu2-O3D	73.74(9)
O12E-Eu2-O3D	69.44(11)
O12F-Eu2-O3D	119.33(11)
O3-Eu2-O3D	92.43(16)
O7-Eu2-O11E	78.00(12)
O7D-Eu2-O11E	69.17(12)
O4D-Eu2-O11E	137.78(11)
O4-Eu2-O11E	110.02(10)
O12E-Eu2-O11E	49.88(10)
O12F-Eu2-O11E	118.66(10)
O3-Eu2-O11E	148.36(11)
O3D-Eu2-O11E	106.62(10)
O7-Eu2-O11F	69.17(12)
O7D-Eu2-O11F	78.00(12)
O4D-Eu2-O11F	110.02(10)
O4-Eu2-O11F	137.78(11)
O12E-Eu2-O11F	118.66(10)
O12F-Eu2-O11F	49.88(10)
O3-Eu2-O11F	106.62(10)
O3D-Eu2-O11F	148.36(11)
O11E-Eu2-O11F	69.47(13)

Symmetry codes: A -x+1/2, -y+2, z+1; B x, y, z+1; C -x+1/2, -y+2, z;

D x, -y+5/2, -z+3/2; E -x+1, y+1/2, z+1/2; F -x+1, -y+2, -z+1

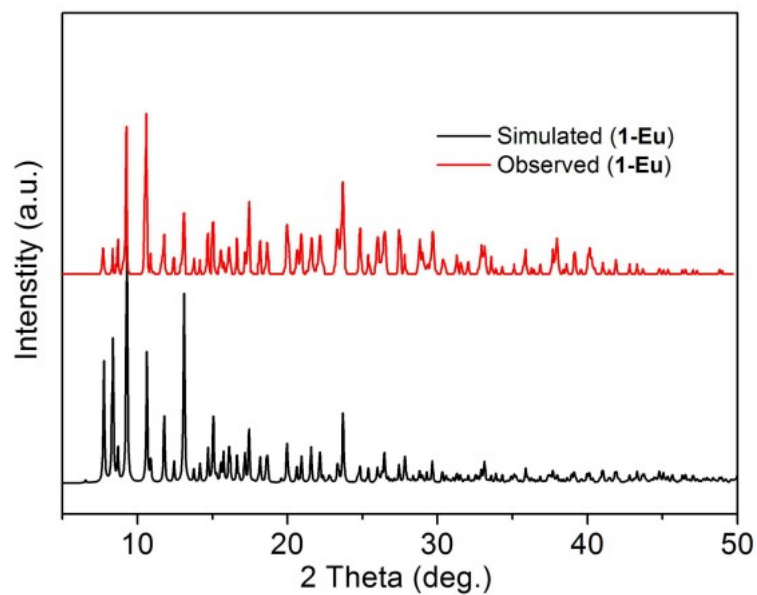


Fig. S1 PXRD data as well as the simulated ones for **1-Eu**.

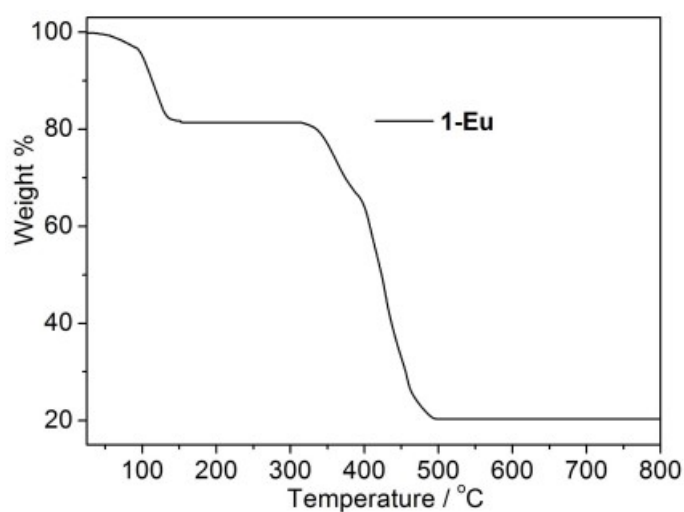


Fig. S2 TGA plots of **1-Eu** under air atmosphere

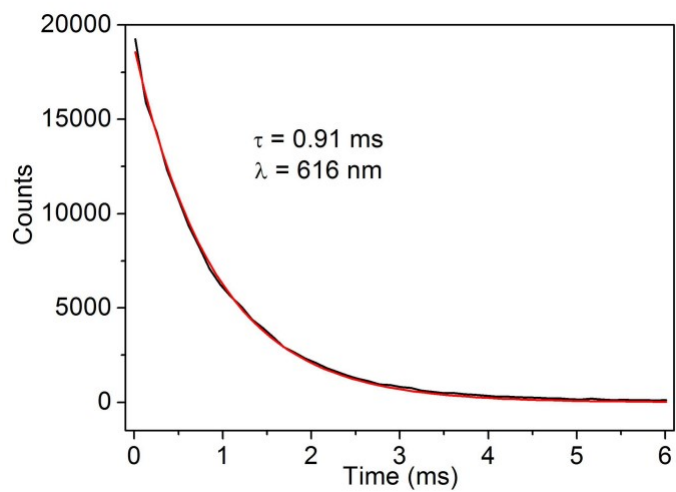


Fig. S3 Emission decay curves of **1-Eu**.

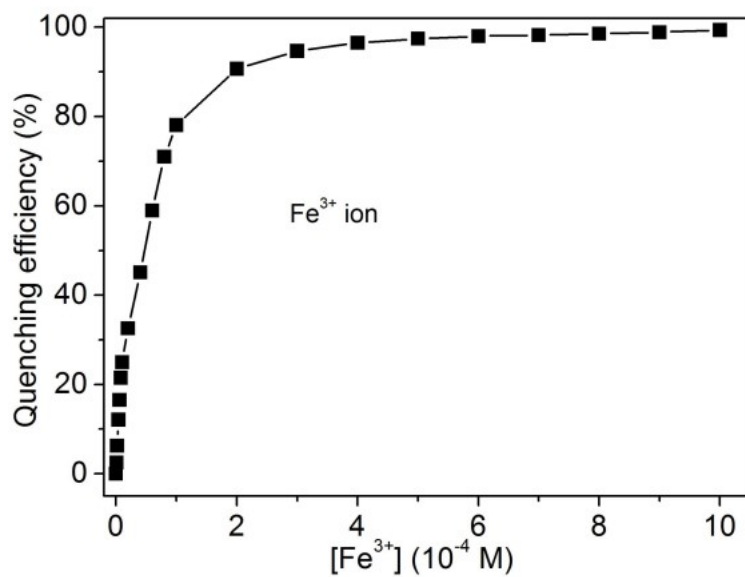


Fig. S4 Quenching efficiency of **1-Eu** dispersed in H_2O with the addition of Fe^{3+} solution.

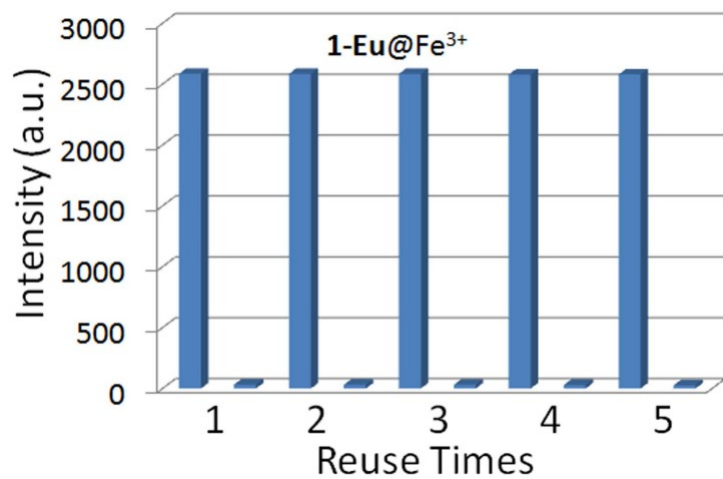


Fig. S5 Repeatability of the quenching ability of **1-Eu** in H₂O and in the presence of Fe³⁺ (1 mM) ($\lambda_{\text{ex}} = 322$ nm).

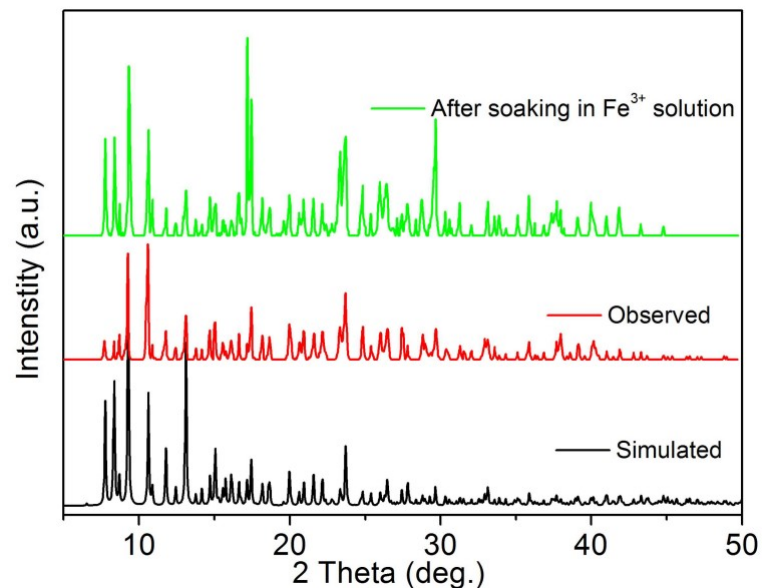


Fig. S6 PXRD patterns of **1-Eu** after soaking in Fe³⁺ solutions.

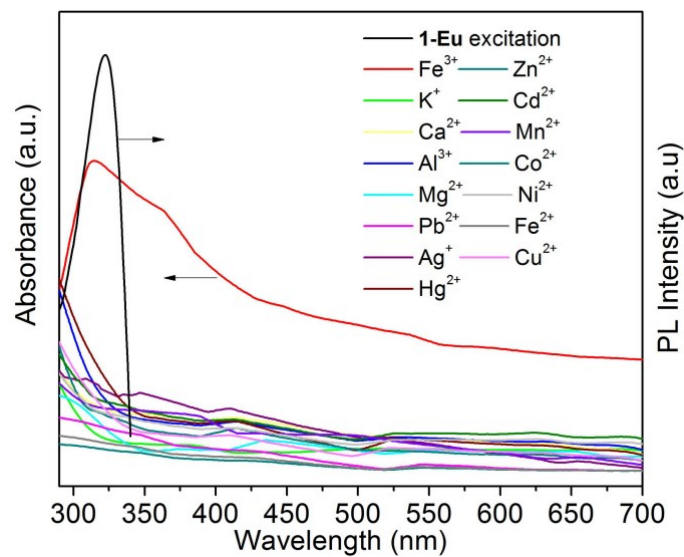


Fig. S7 UV-Vis adsorption spectrum of **1-Eu@cations** aqueous solution with the same concentration of 1×10^{-4} mol·L⁻¹ and the excitation spectrum of **1-Eu**.

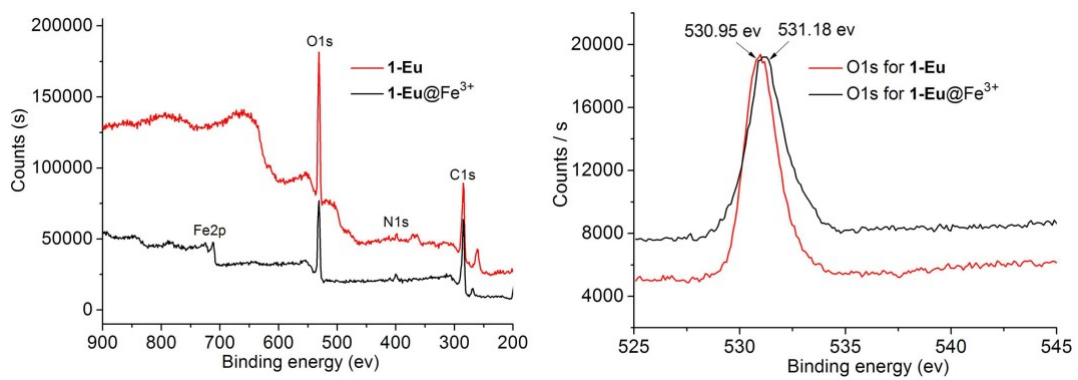


Fig. S8 Comparison of the XPS spectra of 1-Eu before and after treatment with Fe^{3+} ions: overall spectra (left) and O 1s (right).

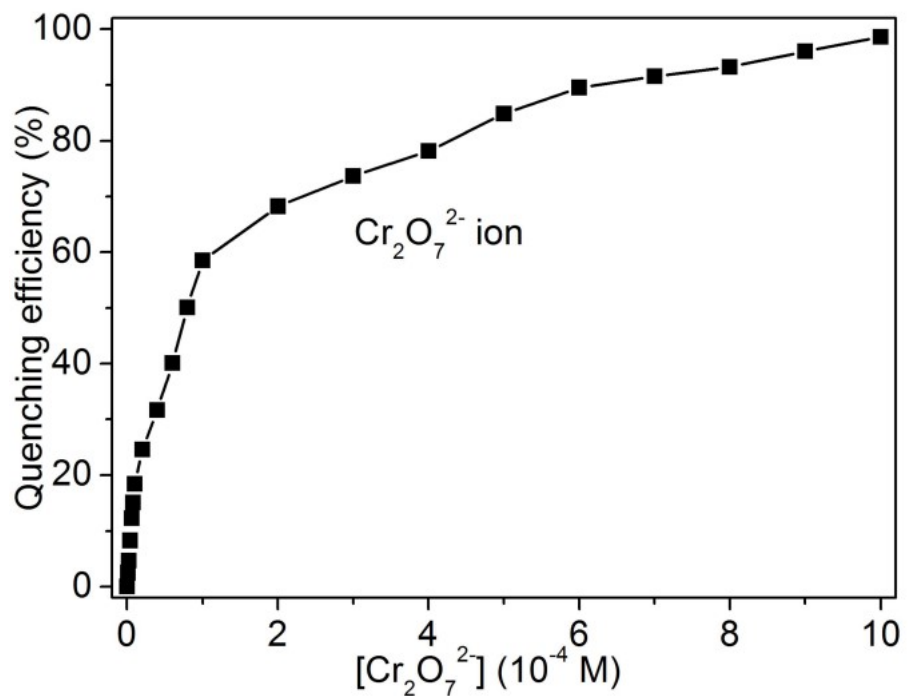


Fig. S9 Quenching efficiency of 1-Eu dispersed in H_2O with the addition of $\text{Cr}_2\text{O}_7^{2-}$ solution.

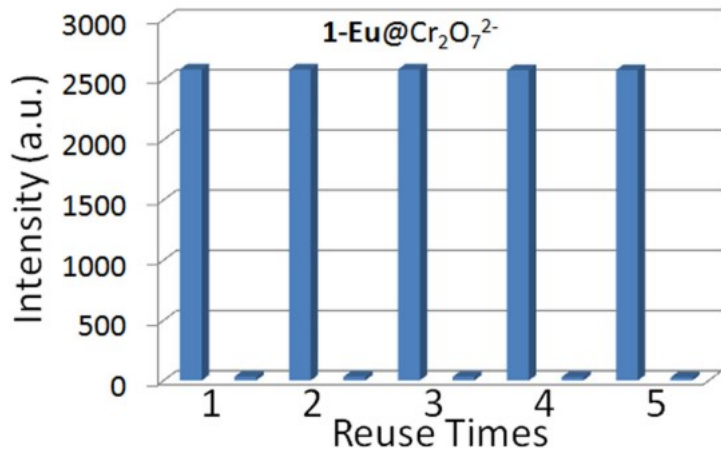


Fig. S10 Repeatability of the quenching ability of **1-Eu** in H₂O and in the presence of Cr₂O₇²⁻ (1 mM) ($\lambda_{\text{ex}} = 322 \text{ nm}$).

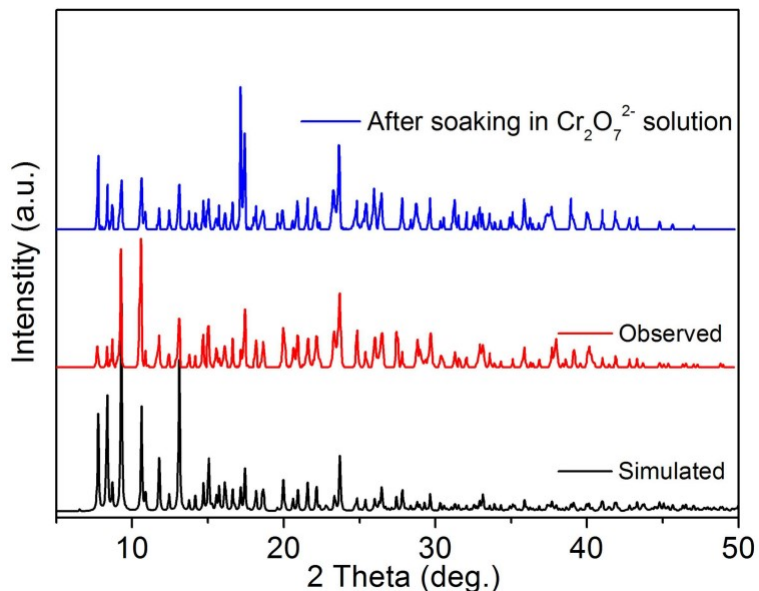


Fig. S11 PXRD patterns of **1-Eu** after soaking in Cr₂O₇²⁻ solutions.

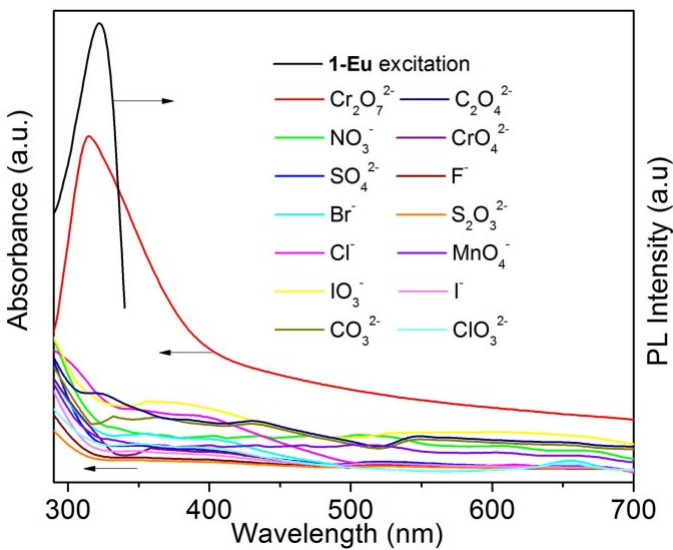


Fig. S12 UV-Vis adsorption spectrum of **1-Eu@anions** aqueous solution with the same concentration of $1 \times 10^{-4} \text{ mol}\cdot\text{L}^{-1}$ and the excitation spectrum of **1-Eu**.

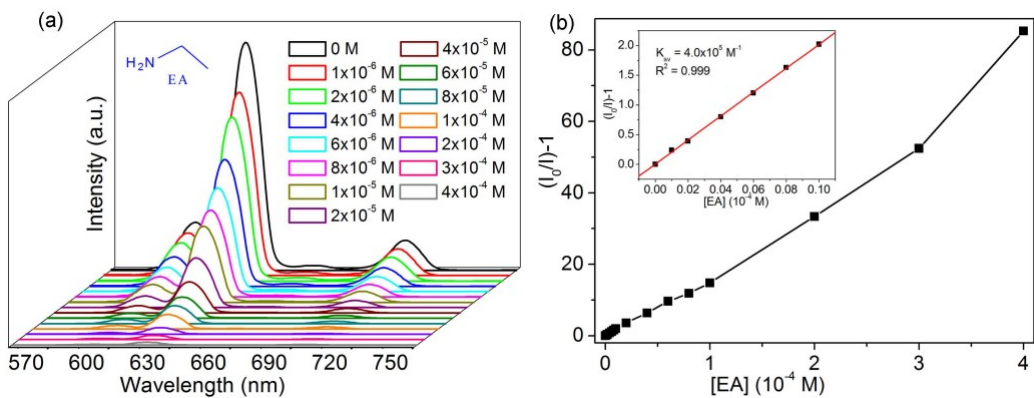


Fig. S13 (a) Emission spectra of **1-Eu** by the gradual addition of EA aqueous solution; (b) The Stern-Volmer plot of **1-Eu** for EA.

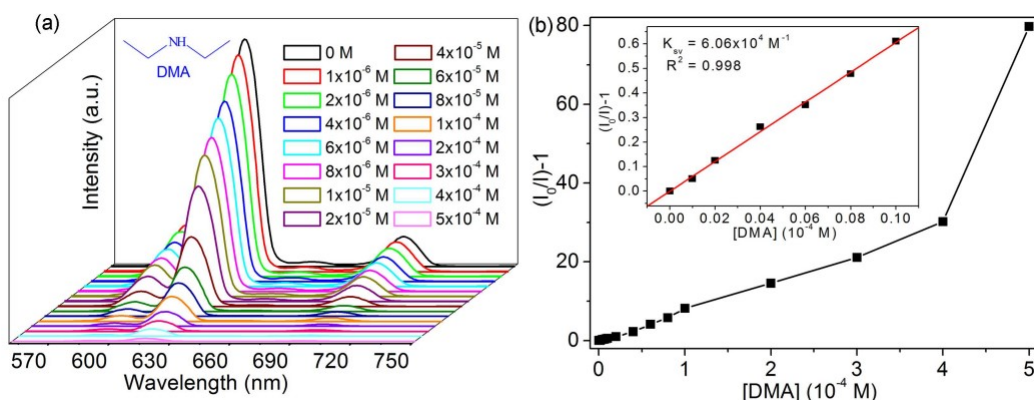


Fig. S14 (a) Emission spectra of **1-Eu** by the gradual addition of DMA aqueous

solution; (b) The Stern-Volmer plot of **1-Eu** for DMA.

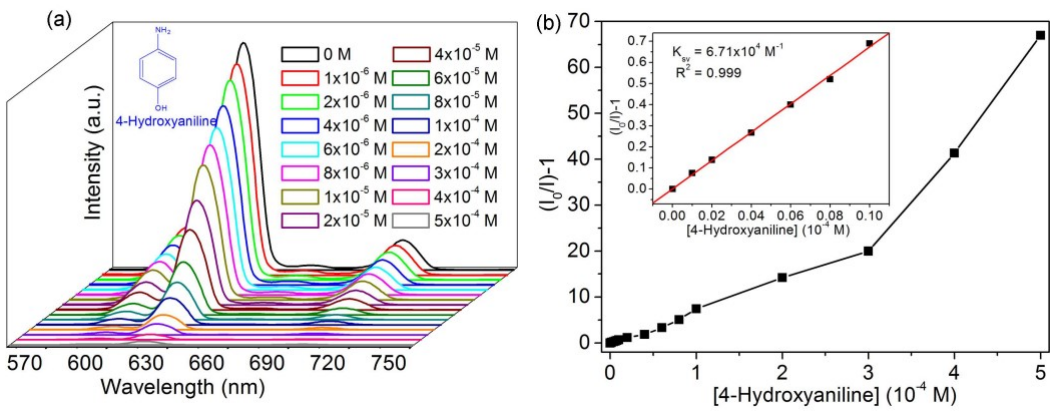


Fig. S15 (a) Emission spectra of **1-Eu** by the gradual addition of 4-Hydroxyaniline aqueous solution; (b) The Stern-Volmer plot of **1-Eu** for 4-Hydroxyaniline.

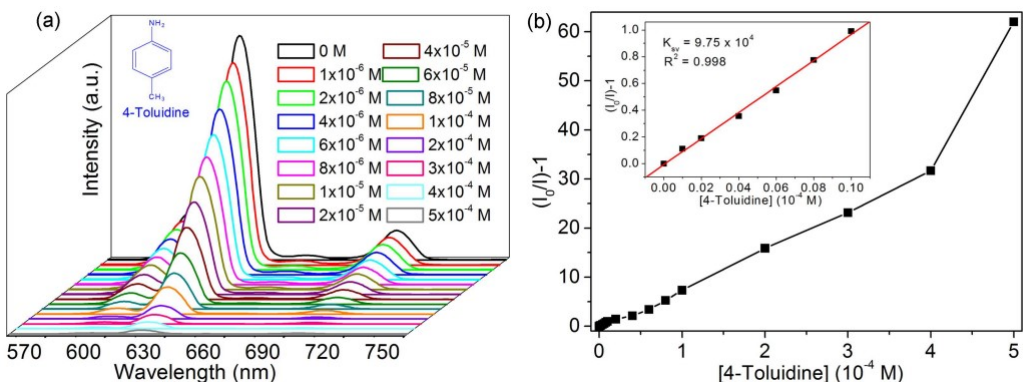


Fig. S16 (a) Emission spectra of **1-Eu** by the gradual addition of 4-Toluidine aqueous solution; (b) The Stern-Volmer plot of **1-Eu** for 4-Toluidine.

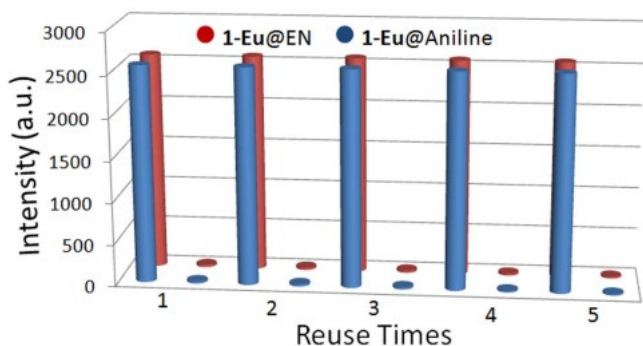


Fig. S17 Repeatability of the quenching ability of **1-Eu** in H_2O and in the presence of

EN (1 mM) and Aniline (1 mM) ($\lambda_{\text{ex}} = 322 \text{ nm}$).

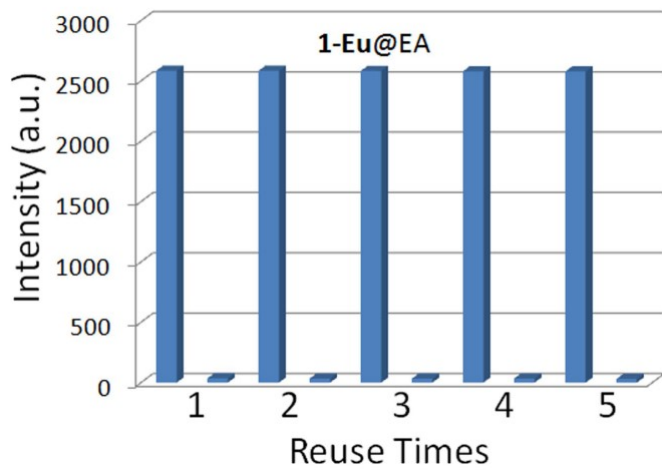


Fig. S18 Repeatability of the quenching ability of **1-Eu** in H_2O and in the presence of EA (1 mM) ($\lambda_{\text{ex}} = 322 \text{ nm}$).

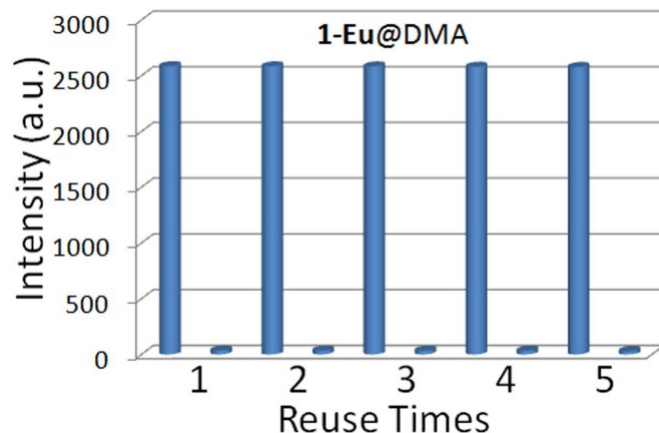


Fig. S19 Repeatability of the quenching ability of **1-Eu** in H_2O and in the presence of DMA (1 mM) ($\lambda_{\text{ex}} = 322 \text{ nm}$).

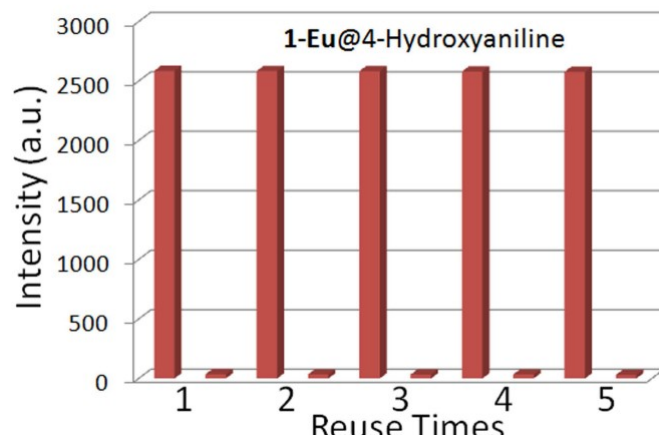


Fig. S20 Repeatability of the quenching ability of **1-Eu** in H_2O and in the presence of

4-Hydroxyaniline (1 mM) (1 mM) ($\lambda_{\text{ex}} = 322 \text{ nm}$).

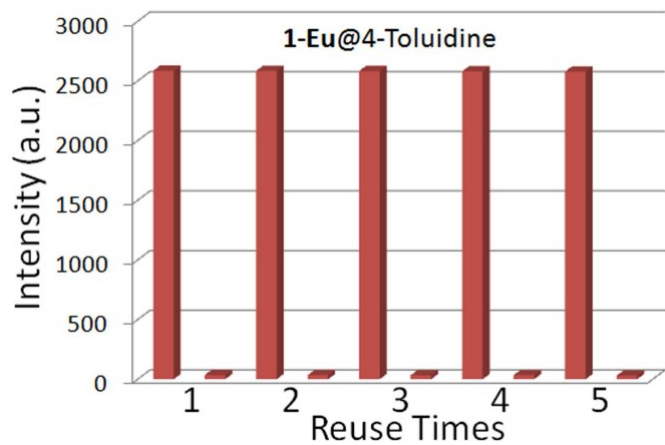


Fig. S21 Repeatability of the quenching ability of **1-Eu** in H_2O and in the presence of 4-Toluidine (1 mM) ($\lambda_{\text{ex}} = 322 \text{ nm}$).

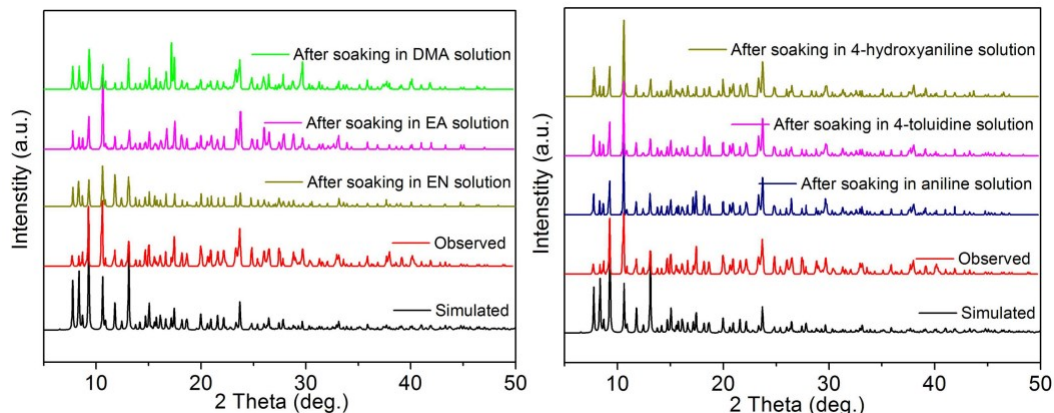


Fig. S22 PXRD patterns of **1-Eu** after soaking in EN, EA, DMA, Aniline, 4-Hydroxyaniline and 4-Toluidine solutions.

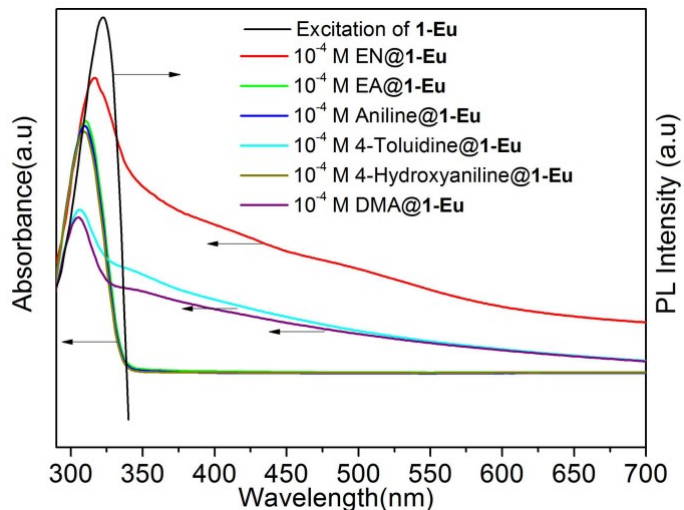


Fig. 23 UV-Vis adsorption spectrum of **1-Eu@amines** aqueous solution with the same concentration of 1×10^{-4} mol·L⁻¹ and the excitation spectrum of **1-Eu**.